

## STRUCTURE NOTE

# The Crystal Structure of Human Muscle Glycogen Phosphorylase $\alpha$ with Bound Glucose and AMP: An Intermediate Conformation with T-State and R-State Features

Christine M. Lukacs,<sup>1\*</sup> Nikos G. Oikonomakos,<sup>3</sup> Robert L. Crowther,<sup>1</sup> Li-Na Hong,<sup>2</sup> R. Ursula Kammlott,<sup>1</sup> Wayne Levin,<sup>2</sup> Shirley Li,<sup>2</sup> Chao-Min Liu,<sup>2</sup> Debra Lucas-McGady,<sup>2</sup> Sherrie Pietranico,<sup>1</sup> and Linda Reik<sup>2</sup>

<sup>1</sup>Roche Pharmaceuticals, Discovery Chemistry, F. Hoffmann-La Roche, Nutley, New Jersey

<sup>2</sup>Roche Pharmaceuticals, Roche Discovery Technologies, F. Hoffmann-La Roche, Nutley, New Jersey

<sup>3</sup>Institute of Organic and Pharmaceutical Chemistry, The National Hellenic Research Foundation, Athens, Greece

**Introduction.** Glycogen phosphorylase (GP) reversibly catalyzes the release of a single glucose-1-phosphate (G-1-P) molecule from glycogen. G-1-P is then converted to glucose via glycolysis in the muscle and via glycogenolysis and gluconeogenesis in the liver. GP is therefore important for the regulation of serum glucose levels, which are elevated in diabetic patients. Inhibition of the liver isoform of GP is of pharmaceutical interest as a therapeutic target for the treatment of type 2 diabetes;<sup>1–4</sup> however, such drugs should exhibit selectivity over the muscle isoform to prevent potential side effects such as muscle cramping due to buildup of glycogen. The human liver and muscle enzymes, which share 79.5% sequence identity, have markedly different kinetic properties; the unphosphorylated (GP<sub>b</sub>) muscle enzyme is completely dependent on the activator AMP for activity, and this activity can be inhibited by ATP or glucose-6-phosphate; the phosphorylated (GP<sub>a</sub>) enzyme is active, and addition of AMP can produce a further 10–20% increase in activity.<sup>5</sup> Liver GP<sub>b</sub> is inactive, and is not sensitive to these effectors; AMP only stimulates liver GP<sub>b</sub> by 10–20%, while liver GP<sub>a</sub> is active and it is not further activated by AMP.<sup>5–7</sup>

GP is a homodimer that exists in either the T (inactive) or R (active) state. Although phosphorylation at Ser 14 normally converts the enzyme to the active R-state, active site and allosteric site binders can modulate the state of the enzyme. Synthetic molecules have been shown by X-ray crystallography to bind GP in the active site,<sup>8,9</sup> the allosteric site,<sup>10–14</sup> the nucleoside inhibitor site,<sup>15–17</sup> and the indole site.<sup>18–22</sup> Over 50 reported structures of GP, mostly of the rabbit muscle or human liver isoform, represent several different states (T, T', R) with different combinations of both natural and synthetic ligands in the various binding sites. Here we report for the first time the expression, purification, crystallization, and crystal structure to 2.3 Å resolution of *human* muscle glycogen phosphorylase  $\alpha$  with both AMP and glucose bound, and describe a previously unobserved conformation that likely represents an intermediate in the transition between the T-state and the R-state.

**Materials and Methods.** Full-length hmGP was cloned by RT-PCR using human muscle mRNA (Clontech) as a template. The cDNA was PCR-amplified using 50× Advantage Polymerase (Clontech). The amplicon was cloned into a pFASTBAC vector. GP was expressed in Sf9 insect cells. After incubation, harvesting, washing, and freeze-thaw, DNAase was added. Cells were sonicated, centrifuged, and the lysate was brought to 300 mM NaCl. Protein was purified via Cu metal affinity, Q Sepharose, and 5'-AMP Sepharose chromatography. The purified GP<sub>b</sub> was incubated with phosphorylase kinase  $\gamma$  subunit 1–300<sup>23</sup> at 5  $\mu$ g/mg GP in the presence of 2.5 mM ATP and 5 mM MgCl<sub>2</sub>. The phosphorylated GP<sub>a</sub> sample was loaded onto a Superdex 200 column equilibrated with 50 mM  $\beta$ -glycerophosphate, 100 mM NaCl, 0.2 mM EDTA, 1 mM DTT, pH 7.5. The final purified GP<sub>a</sub> was concentrated and dialyzed into 20 mM BES, 20 mM NaCl, 1 mM EDTA, 1mM DTT, pH 6.8.

For crystallization, protein at 12 mg/mL + 10 mM AMP was equilibrated against 5% polyethylene glycol monomethyl ether 550, 100 mM glucose, Tris pH 6.9, 2 mM spermine and 4 mM DTT at 4°C. Orthorhombic crystals were transferred through a mixture of reservoir solution with 15% w/v glucose before being cooled in liquid nitrogen. Diffraction data were collected at liquid nitrogen temperature at beamline X8-C at the NSLS at Brookhaven National Laboratories. The crystals diffracted to 2.3 Å resolution and belong to space group P2<sub>1</sub>2<sub>1</sub>2 with unit cell dimensions  $a = 92.4$  Å,  $b = 144.0$  Å,  $c = 59.4$  Å, and contained one protein molecule in the asymmetric unit. The data were processed, scaled, and reduced using the

\*Correspondence to: Christine Lukacs, Roche Pharmaceuticals, Discovery Chemistry, F. Hoffmann-La Roche, 340 Kingsland Street, Nutley, NJ 07110. E-mail: christine.lukacs@roche.com

Received 27 October 2005; Accepted 13 December 2005

Published online 7 March 2006 in Wiley InterScience (www.interscience.wiley.com). DOI: 10.1002/prot.20939

TABLE I. Data Collection and Crystallographic Refinement Statistics

|   |  |
|---|--|
| Data collection   |  |
| Space Group   | P2 <sub>1</sub> 2 <sub>1</sub> 2   |
| Cell constants  | $a = 92.37 \text{ \AA}$ , $b = 144.01 \text{ \AA}$ , $c = 59.44 \text{ \AA}$ |
| Resolution of data  | 2.28 \AA   |
| Number of observations                                      | 124,314  |
| Number of unique reflections                                | 36,521   |
| Completeness (%; last shell)                                | 98.1 (93.1)  |
| Redundancy  | 3.4 (2.94)   |
| $R_{\text{sym}}$ (last shell) <sup>a</sup>                  | 0.068 (0.201)  |
| $I/\sigma(I)$   | 11.4 (5.0)   |
| Refinement  |  |
| Resolution range  | 50.0–2.3 \AA   |
| Number of reflections used in refinement                    | 35,334 (34,628 + 706)  |
| $R_{\text{cryst}}/R_{\text{free}}^b$                        | 0.192/0.251  |
| Number of atoms (protein/water/ligands)                     | 6,707/369/45   |
| Average B-factors ( $\text{\AA}^2$ , protein/water/ligands) | 17.1/19.6/17.3   |
| Rmsd bond lengths (\AA)                                     | 0.006  |
| Rmsd angles (deg)   | 1.4  |

<sup>a</sup> $R_{\text{sym}} = \sum |I_h - \langle I_h \rangle| / \sum I_h$  over all  $h$ , where  $I_h$  is the intensity of reflection  $h$ .

<sup>b</sup> $R_{\text{cryst}}/R_{\text{free}} = \sum ||F_o| - |F_c|| / \sum |F_o|$ .  $R_{\text{free}}$  was calculated with selected reflections excluded from refinement.

HKL2000 package<sup>24</sup> and reindexed using CCP4.<sup>25</sup> Statistics are shown in Table I.

The structure was solved by molecular replacement using the program AMoRe.<sup>26</sup> The A molecule from the crystal structure of R-state rabbit muscle GPb (PDB code 7GPB<sup>27</sup>) was used as a starting model. After one cycle of rigid body, positional, and *B*-factor refinement using CNX,<sup>28</sup> the structure and maps were examined using the program O.<sup>29</sup> The 22 amino acid changes between rabbit and human muscle GP were incorporated. Several loops were removed for rebuilding and/or rebuilt at this time. After one cycle of slow-cool refinement, AMP, glucose, and PLP were added to the structure. After several further rounds of refinement and rebuilding, the final structure contained residues 2–17, 22–249, 261–836, glucose, AMP, and 369 waters. Density at the nucleoside binding site was modeled as the adenine portion of AMP. Lysine 680 is modified by PLP, and Serine 14 is phosphorylated. Residues 548–561 are modeled but are in poor density.

**Results and Discussion.** Although the activator AMP was required to bring the solution of GP to crystallization concentration, crystals were obtained only when the inhibitor glucose was also present in the experiment. Overall, the phosphorylated protein with glucose bound in the active site and AMP bound in the allosteric site [Fig. 1(a)] adopts a conformation that we feel represents an intermediate in the transition between the T- and R-states. Glucose bound at the active site results in much of the protein adopting a T-state conformation, including the overall dimer relationship. However, features such as the ordering of the N-terminus, the binding of AMP in the allosteric site, and the dimeric contacts at the interface near this site are consistent with the R-state conformation. In addition, the 313–325 loop is ordered around the bound AMP in a conformation only previously reported for AMP activated (R-state) GPb with pyridoxal pyrophosphate bound in place of the natural cofactor PLP,<sup>30</sup> resulting in a large and very specific set of contacts between AMP and the enzyme. The combination of AMP binding and phos-

phorylation of Ser 14 stabilizes the N-terminus and the cap- $\alpha$ 2 helix interface, creating a stable, local R-state conformation in this portion of the protein that prevents the completion of the transition to T-state initiated by glucose binding.

The major features that have been observed crystallographically for T-state enzyme—tight glucose binding, the conformation of the tower helices, the closed 280s loop gate—are generally maintained in the human muscle structure. The closest structure by C $\alpha$  RMSD calculation is phosphorylated rabbit muscle GPa with only glucose bound (2GPA;<sup>31</sup> 0.425 \AA for the monomer, 0.653 \AA for the dimer), closer even than rabbit muscle GPa with both glucose and the allosteric site inhibitor W1807 (3AMV<sup>31</sup>) bound. Interestingly, the human liver enzyme with the same combination of ligands (AMP and glucose) bound maintains the R-state conformation (1FA9<sup>6</sup>).

On the other hand, the ordering of the N-terminus, normally observed in phosphorylated enzyme (usually R-state) is found in this structure as well. Residues 2–16 are clearly visible, although there is poor density for residues 17–21, and the side chain of Arg 2 forms a salt link to Glu 8. The phosphoserine is clearly visible, making direct hydrogen bonds to the side chains of Arg 69 and Arg 43'. In contrast, the N-terminus is completely disordered in other T-state GP structures, and modeled with high *B*-factors in T'-state structures.<sup>15,31</sup>

AMP is bound in the versatile allosteric site [Fig. 1(b)], which recognizes a variety of phosphorylated compounds such as IMP, ATP, glucose-6-P,<sup>32</sup> and other nonnatural ligands.<sup>10–14</sup> Contacts made by the liver enzyme to AMP are also found in this structure—namely, hydrogen bonds between the phosphate and Arg 242, Arg 306, Arg 309, Arg 310, Tyr 75, and Tyr 155. There is a face-to-face interaction between the adenine and Tyr 75 and a hydrogen bond between the 2'-OH of the ribose to Asp 42' from the other monomer. Furthermore, the 313–325 loop folds over the nucleoside binding subsite, enclosing the AMP. Hydrogen bonds are formed between the N6 of the AMP and the

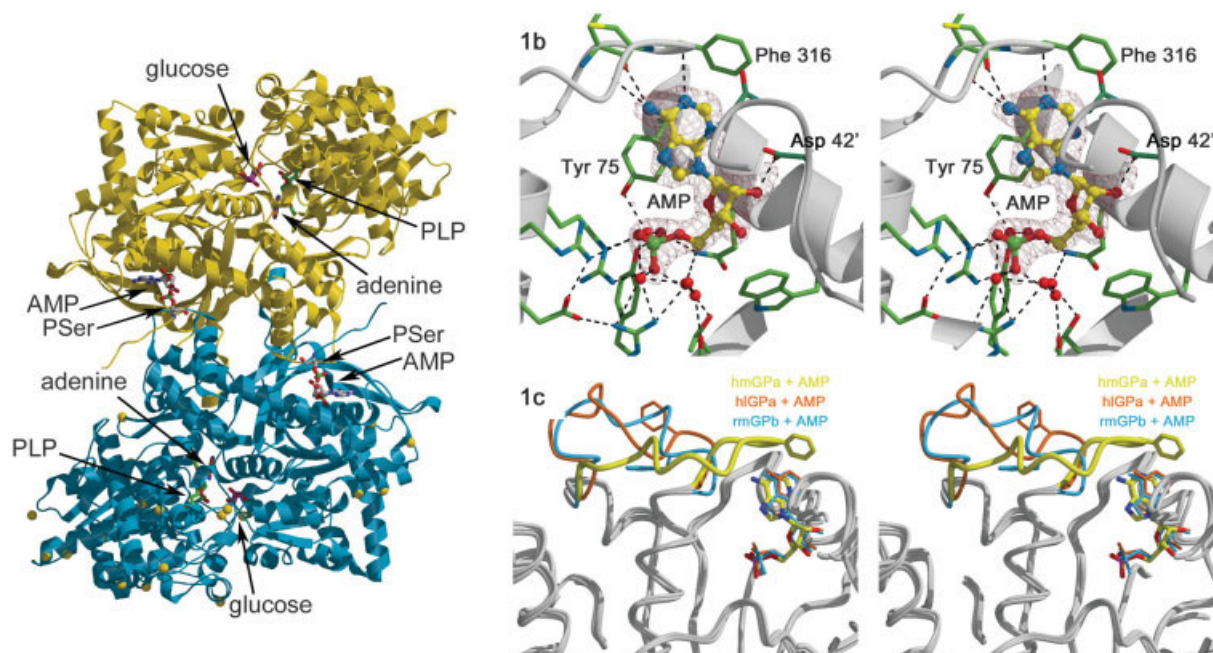


Fig. 1. (a) The overall fold of human muscle glycogen phosphorylase *a*. Because there was one molecule in the asymmetric unit, the active dimer was generated using a symmetry related molecule. Glucose, AMP, PLP, P-Ser 14, and adenine are shown and labeled. The positions of amino acids that differ between the human and rabbit muscle enzyme are shown in the blue monomer as yellow spheres. Figures were made with MOLSCRIPT<sup>35</sup> and Raster3D.<sup>36</sup> (b) Stereoview of the interactions between human muscle GP*a* and AMP. These interactions include extensive water-mediated contacts from the phosphate groups, several direct hydrogen bonds between the adenine and the AMP binding loop, and one hydrogen bond between the ribose and the cap region of the dimeric molecule. Van der Waals contacts from the adenine include an edge-to-face interaction with Phe 316 and a stacking interaction with Tyr 75. 2Fo-Fc density for the AMP is shown at 1 $\sigma$  contour level. (c) Superposition of human muscle glycogen phosphorylase *a* (yellow) with human liver GP*a* with AMP bound (1FA9<sup>6</sup>) in orange and rabbit muscle GP*b* with AMP bound (7GPB<sup>27</sup>) in cyan, highlighting the difference in the allosteric site loop surrounding the AMP. Phe 316 is shown in for the viewer's clarification.

backbone carbonyls of residues Lys 315 and Cys 318, and between N1 and the backbone nitrogen of Gly 317. The side chain of Phe 316 completes this capping by making an edge-to-face interaction with the outer edge of the adenine. This loop is disordered or different in the T or T' state rabbit muscle GP structures,<sup>15,27,31,32</sup> and takes a different path in the liver GP*a*-AMP complex<sup>6</sup> as well. The different conformation of the 313–325 loop in the two isoforms [Fig. 1(c)] may help explain the much higher cooperativity of activation by AMP for the muscle isoform than for the liver isoform.

The rest of the loop is also well defined. Lys 315 forms a salt bridge with symmetry related Glu 785', as does Asp 320 with Lys 786'. Arg 323 reaches back down to the body of the protein to make a salt bridge with Asp 78. These symmetry contacts are not mimicked in the R-state GP*b*-AMP structure,<sup>30</sup> showing that this folding of the adenine binding loop is not a crystallographic artifact, but the true activated structure in the environment of the allosteric site.

The corresponding structure of human liver GP*a* with both AMP and glucose bound has also been solved (1FA9<sup>6</sup>). Rath et al. report that the addition of AMP to liver GP*a* results in crystals that are of the R-state, even when glucose is included in the crystallization setup. Ser 14 phosphorylation and the presence of AMP “set” the conformation of the liver enzyme, and it is not affected by glucose. In contrast, in the human muscle enzyme, the presence of AMP and phosphorylated Ser 14 are unable to prevent glucose from binding and initiating the conversion to T-state. In other words, AMP can

bind to the muscle enzyme even if glucose is bound. The transition to R-state begins, but is stalled until glucose is released, that is, the ease of transition to R-state upon the drop in glucose levels is enhanced.

The implications that this has for drug development are very promising, since antidiabetic drugs should target liver GP. Because there are no sequence differences in the AMP binding site between the liver and muscle isoforms that can be exploited to gain selectivity, one can take advantage of kinetic differences instead. Pfizer has demonstrated that 5-chloroindole based compounds, which bind at the dimer interface, show two- to threefold lower activity against muscle enzyme than liver enzyme.<sup>33,34</sup> It has been shown via crystallography that these compounds bind to and stabilize the T-state of GP.<sup>18,19</sup> Our in-house data (unpublished) additionally show that in the muscle enzyme, these types of compounds are more potent against a glucose-inhibited enzyme, but significantly less potent when both glucose and AMP are present. The T-state of the liver enzyme does not bind AMP; however, we have shown here that T-state muscle enzyme can bind AMP, causing local structural changes—specifically the movements of the  $\alpha$ 2 helix/Val 64, the  $\alpha$ 1 helix, and the 190s loop—which result in a narrowing of the indole binding site that renders it too small for the 5-chloroindole to fit well. Thus, in the physiological state, the indole based inhibitors are clearly better binders to the liver enzyme than the muscle enzyme.

We have demonstrated that the muscle isoform of human

glycogen phosphorylase has structural differences that are consistent with the long-known kinetic differences between the liver and muscle enzymes. The activator AMP can bind the muscle enzyme even when it is locked in the T-state conformation by the binding of glucose. Local changes around the AMP site prime the enzyme for the transition to the R-state, activating it in a way that does not happen in the liver isoform. It will be interesting if future work with this system can elucidate the structures of human muscle GP and human liver GP with an allosteric inhibitor bound. The implications for the enzyme as a target in drug discovery continue to be promising.

## REFERENCES

- Oikonomakos NG. Glycogen phosphorylase as a molecular target for type 2 diabetes therapy. *Curr Protein Pept Sci* 2002;3:561–586.
- BarfT. Intervention of hepatic glucose production. Small molecule regulators of potential targets for Type 2 diabetes therapy. *Mini Rev Med Chem* 2004; 4:897–908.
- Link JT. Pharmacological regulation of hepatic glucose production. *Curr Opin Investig Drugs* 2003;4:421–429.
- Treadway JL, Mendys P, Hoover DJ. Glycogen phosphorylase inhibitors for treatment of type 2 diabetes mellitus. *Exp Opin Invest Drugs* 2001;10:439–444.
- Oikonomakos NG, Acharya KR, Johnson LN. Rabbit muscle glycogen phosphorylase b: structural basis of activation and catalysis. In: Harding JJ, Crabbe MJ, editors. *Post-translational modification of proteins*. Boca Raton, FL: CRC Press; 1992. p 81–151.
- Rath VL, Ammirati M, LeMotte PK, Fennell KF, Mansour MN, Danley DE, Hynes TR, Schulte GK, Wasilko DJ, Pandit J. Activation of human liver glycogen phosphorylase by alteration of the secondary structure and packing of the catalytic core. *Mol Cell* 2000;6:139–148.
- Kobyashi M, Gopalan S, Graves DJ. A comparison of the activator sites of liver and muscle glycogen phosphorylase b. *J Biol Chem* 1982;257:14041–14047.
- Oikonomakos NG, Kosmopoulou M, Zographos SE, Leonidas DD, Chrysina ED, Somsak L, Nagy V, Praly J-P, Docsa T, Toth B, Gergely P. Binding of *N*-acetyl-*N'*- $\beta$ -D-glucopyranosyl urea and *N*-benzoyl-*N'*- $\beta$ -D-glucopyranosyl urea to glycogen phosphorylase b. *Eur J Biochem* 2002;269:1684–1696.
- Somsak L, Nagy V, Haday Z, Docsa T, Gergely P. Glucose analog inhibitors of glycogen phosphorylases as potential antidiabetic agents: recent developments. *Curr Pharm Des* 2003;9:1177–1189.
- Zographos SE, Oikonomakos NG, Tsitsanou KE, Leonidas DD, Chrysina ED, Skamnaki VT, Bischoff H, Goldmann S, Watson KA, Johnson LN. The structure of glycogen phosphorylase b with an alkyl dihydropyridine-dicarboxylic acid compound, a novel and potent inhibitor. *Structure* 1997;5:1413–1425.
- Lu Z, Bohn J, Bergeron R, Deng Q, Ellsworth KP, Geissler WM, Harris G, McCann PE, McKeever B, Myers RW, Saperstein R, Willoughby CA, Yao J, Chapman K. A new class of glycogen phosphorylase inhibitors. *Bioorg Med Chem Lett* 2003;13:4125–4128.
- Ogawa AK, Willoughby CA, Bergeron R, Ellsworth KP, Geissler WM, Myers RW, Yao J, Harris G, Chapman KT. Glucose-lowering in a db/db mouse model by dihydropyridine diacid glycogen phosphorylase inhibitors. *Bioorg Med Chem Lett* 2003;13:3405–3408.
- Kristiansen M, Andersen B, Iversen LF, Westergaard N. Identification, synthesis, and characterization of new glycogen phosphorylase inhibitors binding to the allosteric AMP site. *J Med Chem* 2004;47:3537–3545.
- Klabunde T, Wendt KU, Kadereit D, Brachvogel V, Burger H-J, Herling AW, Oikonomakos NG, Kosmopoulou MN, Schmoll D, Sarubbi E, von Roedern E, Schonafinger K, Defossa E. Acyl ureas as human liver glycogen phosphorylase inhibitors for the treatment of Type 2 diabetes. *J Med Chem*, 2005;48:6178–6193.
- Tsitsanou KE, Skamnaki VT, Oikonomakos NG. Structural basis of the synergistic inhibition of glycogen phosphorylase a by caffeine and a potential antidiabetic drug. *Arch Biochem Biophys* 2000;384:245–254.
- Ekstrom JL, Pauly TA, Carty MD, Soeller WC, Culp J, Danley DE, Hoover DJ, Treadway JL, Gibbs EM, Fletterick RJ, Day YS, Myszka DG, Rath VL. Structure–activity analysis of the purine binding site of human liver glycogen phosphorylase. *Chem Biol* 2000;9:915–924.
- Oikonomakos NG, Schnier JB, Zographos SE, Skamnaki VT, Tsitsanou KE, Johnson LN: Flavopiridol inhibits glycogen phosphorylase by binding at the inhibitor site. *J Biol Chem* 2000;275: 34566–34573.
- Rath VL, Ammirati M, Danley DE, Ekstrom JL, Gibbs EM, Hynes TR, Mathiowetz AM, McPherson RK, Olson TV, Treadway JL, Hoover DJ. Human liver glycogen phosphorylase inhibitors bind at a new allosteric site. *Chem Biol* 2000;7:677–682.
- Oikonomakos NG, Skamnaki VT, Tsitsanou KE, Gavalas NG, Johnson LN. A new allosteric site in glycogen phosphorylase b as a target for drug interactions. *Structure* 2000;8:575–584.
- Oikonomakos NG, Zographos SE, Skamnaki VT, Archontis G. The 1.76 Å resolution crystal structure of glycogen phosphorylase B complexed with glucose, and CP320626, a potential antidiabetic drug. *Bioorg Med Chem* 2002;10:1313–1319.
- Rosauer KG, Ogawa AK, Willoughby CA, Ellsworth KP, Geissler WM, Myers RW, Deng Q, Chapman KT, Harris G, Moller DE. Novel 3,4-dihydroquinolin-2(1H)-one inhibitors of human glycogen phosphorylase a. *Bioorg Med Chem Lett* 2003;13:4385–4388.
- Wright SW, Rath VL, Genereux PE, Hageman DL, Levy CB, McClure LD, McCoid SC, McPherson RK, Schelhorn TM, Wilder DE, Zavadoski WJ, Gibbs EM, Treadway JL. 5-Chloroindoloyl glycine amide inhibitors of glycogen phosphorylase: synthesis, *in vitro*, *in vivo*, and X-ray crystallographic characterization. *Bioorg Med Chem Lett* 2005;15:459–465.
- Huang CY, Yuan CJ, Livanova NB, Graves DJ. Expression, purification, characterization, and deletion mutations of phosphorylase kinase gamma subunit: identification of an inhibitory domain in the gamma subunit. *Mol Cell Biochem* 1993;127–128:7–18.
- Otwinowski K, Minor W. Processing of X-ray diffraction data collected in oscillation mode. *Methods Enzymol* 1997;276:307–326.
- CCP4. CCP4 Suite: programs for protein crystallography. *Acta Crystallogr D* 1994;50:760–763.
- Navaza J. AMoRe: an automated package for molecular replacement. *Acta Crystallogr A* 2004;A50:157–163.
- Barford D, Hu SH, Johnson LN. Structural mechanism for glycogen phosphorylase control by phosphorylation and AMP. *J Mol Biol* 1991;218:233–260.
- Brunger AT, Adams PD, Clore GM, DeLano WL, Gros P, Grosse-Kunstleve RW, Jiang JS, Kuszewski J, Nilges M, Pannu NS, Read RJ, Rice LM, Simonson T, Warren GL. Crystallography & NMR system: a new software suite for macromolecular structure determination. *Acta Crystallogr D* 1998;54(Pt. 5):905–921.
- Jones AT, Zou JY, Cowan SW, Kjeldgaard M. Improved methods for building protein models in electron density maps and the location of errors in these models. *Acta Crystallogr A* 1991;47:110–119.
- Sprang SR, Withers SG, Goldsmith EJ, Fletterick RJ, Madsen NB. Structural basis for the activation of glycogen phosphorylase b by adenosine monophosphate. *Science* 1991;254:1367–1371.
- Oikonomakos NG, Tsitsanou KE, Zographos SE, Skamnaki VT, Goldmann S, Bischoff H. Allosteric inhibition of glycogen phosphorylase a by the potential antidiabetic drug 3-isopropyl 4-(2-chlorophenyl)-1,4-dihydro-1-ethyl-2-methyl-pyridine-3,5,6-tricarboxylate. *Protein Sci* 1999;8:1930–1945.
- Johnson LN, Snape P, Martin JL, Acharya KR, Barford D, Oikonomakos NG. Crystallographic binding studies on the allosteric inhibitor glucose-6-phosphate to T state glycogen phosphorylase b. *J Mol Biol* 1993;232:253–267.
- Hoover DJ, Lefkowitz-Snow S, Burgess-Henry JL, Martin WH, Armento SJ, Stock IA, McPherson RK, Genereux PE, Gibbs EM, Treadway JL. Indole-2-carboxamide inhibitors of human liver glycogen phosphorylase. *J Med Chem* 1998;41:2934–2938.
- Martin WH, Hoover DJ, Armento SJ, Stock IA, McPherson RK, Danley DE, Stevenson RW, Barrett EJ, Treadway JL. Discovery of a human liver glycogen phosphorylase inhibitor that lowers blood glucose *in vivo*. *Proc Natl Acad Sci USA* 1998;95:1776–1781.
- Kraulis PJ. MOLSCRIPT: a program to produce both detailed and schematic plots of protein structures. *J Appl Crystallogr* 1991;24: 946–950.
- Merritt EA, Bacon DJ. Raster3D photorealistic molecular graphics. *Methods Enzymol* 1997;277:505–524.